

Lateral dynamics of a bicycle with passive rider model

A. L. Schwab^N and J. D. G. Kooijman^N

^N Laboratory for Engineering Mechanics
Delft University of Technology
Mekelweg 2, NL 2628 CD Delft, The Netherlands
Phone: +31-15-2782701, Fax: +31-15-2782150
email: a.l.schwab@tudelft.nl
email: jodikooijman@gmail.com

ABSTRACT

This paper addresses the influence of a passive rider on the lateral dynamics of a Whipple-like bicycle model. In the original Whipple [8] model the rider is assumed to be rigidly connected to the rear frame of the bicycle and there are no hands on the handlebar. Contrary, in normal bicycling the arms of a rider are connected to the handlebar and the rider can use both steering and upper body rotations for control. From observations [2, 6] two distinct rider postures can be identified. The first posture is where the upper body leans forward with the arms stretched to the handlebar, and the upper body twists while steering. The second rider posture is an upright one where the upper body stays fixed with respect to the rear frame and where the arms, hinging at the shoulders and the elbows, exert the control force on the steering. Models can be made where neither posture adds any degrees of freedom to the original Whipple-like bicycle model. For both posture cases the open loop, or uncontrolled, dynamics of the bicycle-rider system is investigated and compared to the rigid rider model by examining the eigenvalues and eigenmotions in the 0 to 10 m/s forward speed range. It is shown that such a passive rider can dramatically change the eigenvalues and its structure with respect to those of the rigid rider model.

Keywords: Bicycle dynamics, human control, nonholonomic systems, multibody dynamics.

1 INTRODUCTION

The bicycle is an intriguing machine as it is laterally unstable at low speed and stable, or easy to stabilize, at high speed. During the last decade a revival in the research on dynamics and control of bicycles has taken place [4]. Most studies use the so-called Whipple model [8] of a bicycle. In this model a hands-free rigid rider is fixed to the rear frame. However, from experience it is known that some form of control is required to stabilize the bicycle and/or carry out tracking operations. This control is either done by steering or by performing some set of upper body motions. The precise control used by the rider is currently under study [2, 6]. Here we focus on steering and the contribution of passive body motions on the uncontrolled dynamics of a bicycle. In a previous study [7] it has been shown that passive lateral upper-body motions have little effect on the uncontrolled dynamics of a bicycle.

From observations [2, 6] two distinct rider postures can be identified. The first posture is where the upper body leans forward with the arms stretched to the handlebar, and the upper body twists while steering, as can be seen in Figure 1a. The second rider posture is an upright one where the upper body stays fixed with respect to the rear frame and where the arms, hinging at the shoulders and the elbows, exert the control force on the steering, shown in Figure 1b. Models can be made where neither posture adds any degrees of freedom to the original Whipple-like bicycle model. For both posture cases the open loop, or uncontrolled, dynamics of the bicycle-rider system is investigated and compared to the rigid rider model by examining the eigenvalues and eigenmotions in the 0 to 10 m/s forward speed range. The paper is organized as follows. First the original bicycle model is presented. Next the extension of this model with a twisting upper body or flexed arms is presented and the stability of the lateral motions are compared to those of a rigid rider model. The paper ends with some conclusions.



(a) Rider A on the Stratos bicycle



(b) Rider A on the Browser bicycle

Figure 1: Bicycling on a treadmill, two distinct postures: **a)** Rider A on the Stratos bicycle with forward leaned body and stretched arms. **b)** Rider A on the Browser bicycle with an upright body and flexed arms.

2 BICYCLE MODEL

The basic bicycle model used is the so-called Whipple [8] model which recently has been benchmarked [4]. The model, see Figure 2, consists of four rigid bodies connected by revolute joints. The contact between the knife-edge wheels and the flat level surface is modelled by holonomic constraints in the normal direction and by non-holonomic constraints in the longitudinal and lateral direction. In this original model it is assumed that the rider is rigidly attached to the rear frame and has no hands on the handlebar. The resulting non-holonomic mechanical model has three velocity degrees of freedom: forward speed v , lean rate $\dot{\phi}$ and steering rate $\dot{\delta}$.

For the stability analysis of the lateral motions we consider the linearized equations of motion for small perturbations about the upright steady forward motion. These linearized equations of motion are fully described in Meijaard 2007 [4]. They are expressed in terms of small changes in the lateral degrees of freedom.

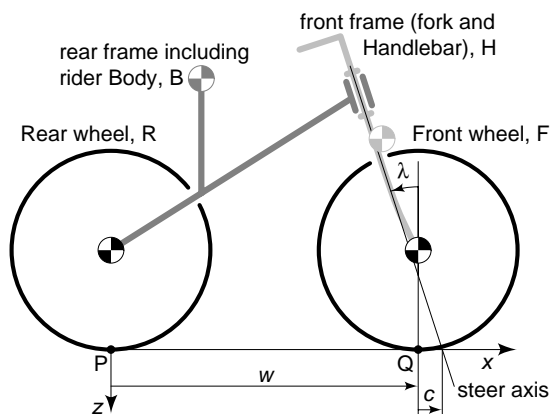


Figure 2: The bicycle model: four rigid bodies (rear wheel R, rear frame B, front handlebar assembly H, front wheel F) connected by three revolute joints (rear hub, steering axis, front hub), together with the coordinate system, and the degrees of freedom.

freedom (the rear frame roll angle, ϕ , and the steering angle, δ) from the upright straight ahead configuration $(\phi, \delta) = (0, 0)$, at a forward speed v , and have the form

$$\mathbf{M}\ddot{\mathbf{q}} + v\mathbf{C}_1\dot{\mathbf{q}} + [g\mathbf{K}_0 + v^2\mathbf{K}_2]\mathbf{q} = \mathbf{f}, \quad (1)$$

where the time-varying variables are $\mathbf{q} = [\phi, \delta]^T$ and the lean and steering torques $\mathbf{f} = [T_\phi, T_\delta]^T$. The coefficients in this equation are: a constant symmetric mass matrix, \mathbf{M} , a damping-like (there is no real damping) matrix, $v\mathbf{C}_1$, which is linear in the forward speed v , and a stiffness matrix which is the sum of a constant symmetric part, $g\mathbf{K}_0$, and a part, $v^2\mathbf{K}_2$, which is quadratic in the forward speed. The forces on the right-hand side, \mathbf{f} , are the applied forces which are energetically dual to the degrees of freedom \mathbf{q} .

The entries in the constant coefficient matrices \mathbf{M} , \mathbf{C}_1 , \mathbf{K}_0 , and \mathbf{K}_2 can be calculated from a non-minimal set of 25 bicycle parameters as described in Meijaard 2007 [4]. A procedure for measuring these parameters for a real bicycle is described in [3], where measured values for the bicycles used in this study can be found in Table 2. Then, with the coefficient matrices the characteristic equation,

$$\det(\mathbf{M}\lambda^2 + v\mathbf{C}_1\lambda + g\mathbf{K}_0 + v^2\mathbf{K}_2) = 0, \quad (2)$$

can be formed and the eigenvalues, λ , can be calculated. These eigenvalues, in the forward speed range of $0 \leq v \leq 10$ m/s, are presented for example for the Stratos bicycle with a rigid rider in Figure 4a. In principle there are up to four eigenmodes, where oscillatory eigenmodes come in pairs. Two are significant and are traditionally called the *capsize mode* and *weave mode*. The capsize mode corresponds to a real eigenvalue with eigenvector dominated by lean: when unstable, the bicycle just falls over like a capsizing ship. The weave mode is an oscillatory motion in which the bicycle sways about the headed direction. The third remaining eigenmode is the overall stable *castering mode*, like in a caster wheel, which corresponds to a large negative real eigenvalue with eigenvector dominated by steering.

At near-zero speeds, typically $0 < v < 0.5$ m/s, there are two pairs of real eigenvalues. Each pair consists of a positive and a negative eigenvalue and corresponds to an inverted-pendulum-like falling of the bicycle. The positive root in each pair corresponds to falling, whereas the negative root corresponds to the time reversal of this falling. When speed is increased two real eigenvalues coalesce and then split to form a complex conjugate pair; this is where the oscillatory weave motion emerges. At first this motion is unstable but at $v_w \approx 4.7$ m/s, the *weave speed*, these eigenvalues cross the imaginary axis in a Hopf bifurcation and this mode becomes stable. At a higher speed the capsize eigenvalue crosses the origin in a pitchfork bifurcation at $v_c \approx 7.9$ m/s, the *capsize speed*, and the bicycle becomes mildly unstable. The speed range for which the uncontrolled bicycle shows asymptotically stable behaviour, with all eigenvalues having negative real parts, is $v_w < v < v_c$.

3 PASSIVE RIDER MODELS

The original Whipple model can be extended with a passive rider. From observations where riding on a large treadmill (3×5 m) [2, 6], two distinct postures emerged which will be modeled. In the first posture model the upper body is leaned forward and the arms are stretched and connected to the handlebar whereas the upper body is allowed to twist, see Figure 3a. The second posture model has a rigid upper body connected to the rear frame and hinged arms at the shoulder and elbow connected to the handlebar, see Figure 3b. Neither model adds any extra degree of freedom to the original Whipple model. This means that the number and structure of the linearized equations of motion (1) stays the same, only the entries in the matrices change.

For the modelling of the geometry and mass properties of the rider, the method as described by Moore *et al.* 2009 [5] is used. Here the human rider is divided into a number of simple geometric objects like cylinders, blocks and a sphere of constant density see Figure 6a. Then with the proper dimensions and the estimates of the individual body part masses the mechanical models can be made. For rider A used in this study this data can be found in Table 3, whereas the calculation of the necessary skeleton points is given in Table 4.

The geometry and mass properties of the two bicycles used in this study were measured by the procedure as described in [3] and the results are presented in Table 2.

The complete model of the bicycle with passive rider was analyzed with the multibody dynamics software package SPACAR [1]. SPACAR handles systems of rigid and flexible bodies connected by various joints

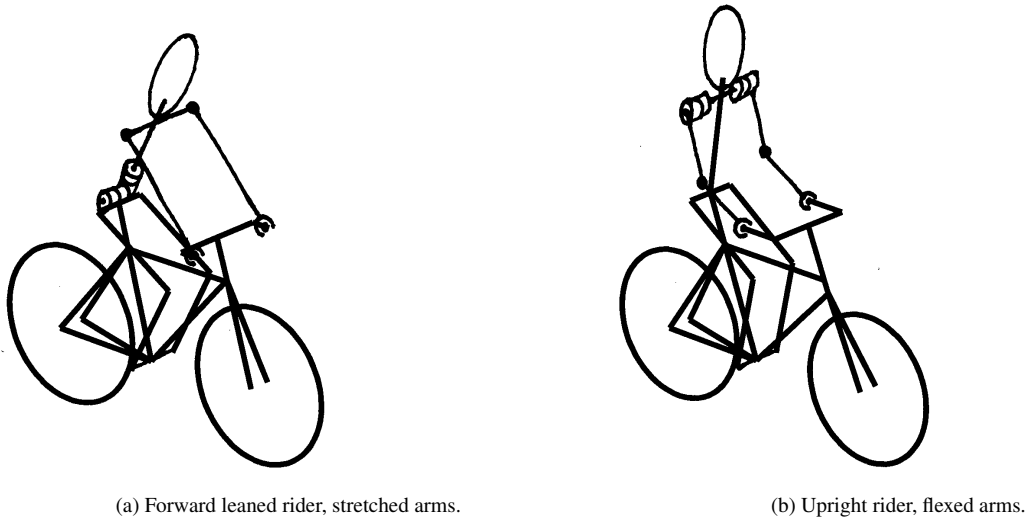


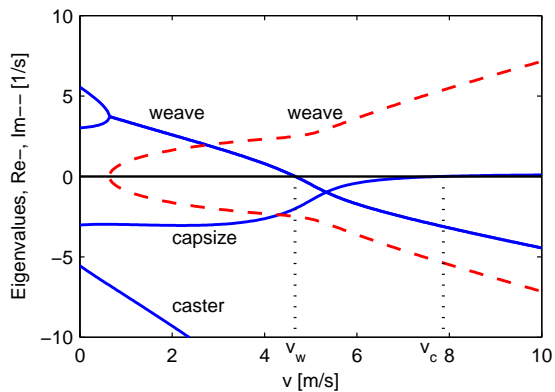
Figure 3: Two distinct bicycle models which include a passive rider: **a)** Rider with forward leaned body and stretched arms. **b)** Rider with upright body and flexed arms.

in both open and closed kinematic loops, and where parts may have rolling contact. SPACAR generates numerically, and solves, full non-linear dynamics equations using minimal coordinates (constraints are eliminated). SPACAR can also find the numeric coefficients for the linearized equations of motion based on a semi-analytic linearization of the non-linear equations. This technique has been used here to generate the constant coefficient matrices \mathbf{M} , \mathbf{C}_1 , \mathbf{K}_0 , and \mathbf{K}_2 from the linearized equations of motion (1) which serve as a basis for generating the eigenvalues of the lateral motions in the desired forward speed range.

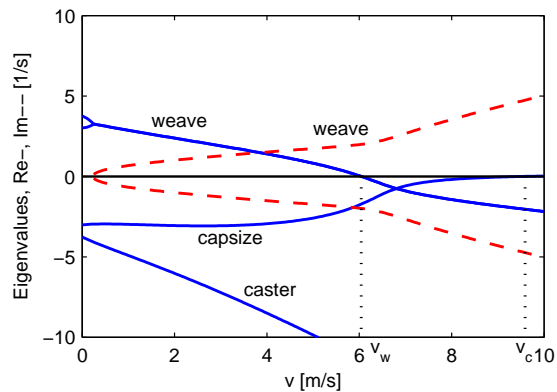
3.1 FORWARD LEANED PASSIVE RIDER

In this posture model the upper body is leaned forward and the arms are stretched and connected to the handlebar, see Figure 3a. The leaned upper body is allowed to twist about its longitudinal axis when steered. The upper body also needs a pitching degree of freedom but in a first order approximation the pitching motions is zero. This also follows directly from symmetry arguments. The linearized equations of motion are derived as described above together with the eigenvalues of the lateral motions. These eigenvalues are shown in Figure 4b. For comparison the eigenvalues for a rigid rider, that is the rider is rigidly attached to the rear frame and there are no hands on the handlebar, are shown in Figure 4a.

Compared to the rigid rider solutions there are some small changes in the eigenvalues but the overall structure is still the same. Most noticeable is that the stable speed range goes up and the the frequency of the weave motion goes down. This can be explained as follows. Adding this passive rider model makes two major changes to a fully rigid rider model. The first is that the attached passive mechanism of arms and twisting upper body adds a mass moment of inertia to the steering assembly. Looking at the entries in the mass matrix this increases the diagonal mass term $M(2, 2)$ for the steering degree of freedom δ , from 0.25 kgm^2 to 0.69 kgm^2 . The off-diagonal terms increase slightly. The effect on the eigenvalues is that the added mass increases the weave speed and decreases the weave frequencies overall. The second change is the added stiffness to the steering assembly due to the compression forces exerted by the hands on the handlebar when leaning forward. This effects more entries in the matrices of the linearized equations of motion which the most noticeable are the changes in the constant symmetric stiffness matrix \mathbf{K}_0 . The diagonal term for the steering stiffness, $K_0(2, 2)$, increases from -6.8 Nm/rad to -3.2 Nm/rad and the off-diagonal terms decrease by 50 %. The effect on the eigenvalues of this increased stiffness is an increased capsiz speed and an overall increase of weave frequencies. However the two effects together, result in little change compared to the rigid rider model as described above. It should also be noted that the more the direction of

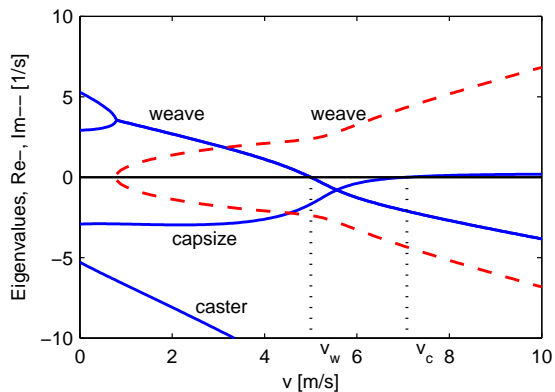


(a) Eigenvalues for the Stratos bicycle with fully rigid rider, hands-free.

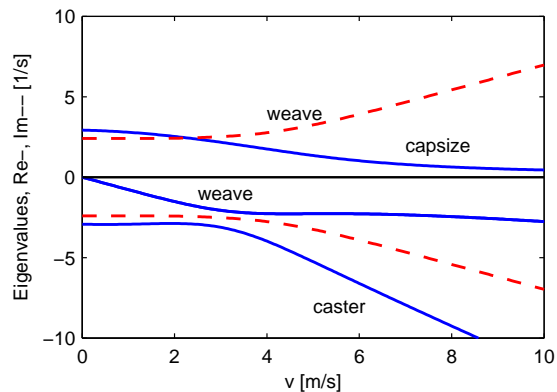


(b) Eigenvalues for the Stratos bicycle with a rider with stretched arms, hands on the handle bars and a yawing upper body.

Figure 4: Eigenvalues for the lateral motions of a bicycle-rider combination with **a)** a fully rigid rider and hands-free; **b)** with a rider with stretched arms, hands on the handle bars and a yawing upper body according to the model from Figure 3a.



(a) Eigenvalues for the Browser bicycle with fully rigid rider and hands-free.



(b) Eigenvalues for the Browser bicycle with a rider with rigid upper body and flexed arms and hands on the handle bars.

Figure 5: Eigenvalues for the lateral motions of a bicycle-rider combination with **a)** a fully rigid rider and hands-free; **b)** with a rider with rigid upper body and flexed arms and hands on the handle bars according to the model from Figure 3b.

the stretched arms is parallel to the steer axis, the less is the change in the dynamics compared to the rigid rider model.

3.2 UPRIGHT PASSIVE RIDER

In the upright posture the rigid upper body is connected to the rear frame and the arms are hinged at the shoulder and elbow and connected via the hands to the handlebar, see Figure 3b. The linearized equations of motion are derived as described above together with the eigenvalues of the lateral motions. These eigenvalues are shown in Figure 5b. For comparison the eigenvalues for a rigid rider, that is the rider is rigidly attached to the rear frame and there are no hands on the handlebar, are shown in Figure 5a.

Compared to the rigid rider solutions there are dramatic changes in the eigenvalue structure. The stable forward speed range has disappeared completely because the weave speed has decreased to zero and the capsize motion is always unstable. Note that the weave motion is now always stable but gets washed out by the unstable capsize. This dramatic change can be explained as follows. By adding the hinged arms to the handlebar a stable pendulum-type of oscillator has been added to the steer assembly. Although this

oscillator stabilizes the initial unstable weave motion it kills the stable eigen-dynamics of the bicycle. The steer assembly is not able to stabilize the lateral motion by the steer-into-the fall mechanism. The added mass is most noticeable in the diagonal steering related term $M(2, 2)$ which increases from 0.25 kgm^2 to 0.46 kgm^2 . More dramatic is the change in the constant symmetric stiffness matrix \mathbf{K}_0 , here the steering related stiffness $K_0(2, 2)$ increase from an unstable -6.6 Nm/rad to a stable 2.3 Nm/rad , which partly explains the dramatic change in the eigenvalue structure.

4 CONCLUSIONS

Adding a passive upper body to the three degree of freedom Whipple model of an uncontrolled bicycle, without adding any extra degrees of freedom, can change the open-loop dynamics of the system. In the case of a forward leaned rider with stretched arms and hands on the handle bars there is little change. However, an upright rider position with flexed arms and hands on the handle bars changes the open-loop dynamics drastically and ruins the self stability of the system.

Future work is direct towards the comparison of the control effort of the human rider in both postures.

ACKNOWLEDGEMENT

Thanks to Jason Moore for measuring the bicycles and riders during his Fulbright granted year (2008/2009) at TUDelft and thanks to Batavus for supplying the bicycles.

REFERENCES

- [1] JONKER, J. B., AND MEIJAARD, J. P. SPACAR - Computer program for dynamic analysis of flexible spatial mechanisms and manipulators. In *Multibody systems handbook* (1990), W. Schiehlen, Ed., Berlin, Germany: Springer, pp. 123–143.
- [2] KOUIJMAN, J. D. G., AND SCHWAB, A. L. Some observations on human control of a bicycle. In *11th mini Conference on Vehicle System Dynamics, Identification and Anomalies (VSDIA2008)*, Budapest, Hungary (Nov. 2008), I. Zobory, Ed., Budapest University of Technology and Economics, p. 8.
- [3] KOUIJMAN, J. D. G., SCHWAB, A. L., AND MEIJAARD, J. P. Experimental validation of a model of an uncontrolled bicycle. *Multibody System Dynamics* 19 (2008), 115–132.
- [4] MEIJAARD, J. P., PAPADOPOULOS, J. M., RUINA, A., AND SCHWAB, A. L. Linearized dynamics equations for the balance and steer of a bicycle: a benchmark and review. *Proceedings of the Royal Society A* 463 (2007), 1955–1982.
- [5] MOORE, J. K., HUBBARD, M., KOUIJMAN, J. D. G., AND SCHWAB, A. L. A method for estimating physical properties of a combined bicycle and rider. In *Proceedings of the ASME 2009 International Design Engineering Technical Conferences & Computers and Information in Engineering Conference (DETC2009)*, Aug 30 – Sep 2, 2009, San Diego, CA, 2009).
- [6] MOORE, J. K., KOUIJMAN, J. D. G., AND SCHWAB, A. L. Rider motion identification during normal bicycling by means of principal component analysis. In *MULTIBODY DYNAMICS 2009, ECCOMAS Thematic Conference* (29 June–2 July 2009, Warsaw, Poland, 2009), M. W. K. Arczewski, J. Fraczek, Ed.
- [7] SCHWAB, A. L., KOUIJMAN, J. D. G., AND MEIJAARD, J. P. Some recent developments in bicycle dynamics and control. In *Fourth European Conference on Structural Control (4ECSC)* (2008), A. K. Belyaev and D. A. Indeitsev, Eds., Institute of Problems in Mechanical Engineering, Russian Academy of Sciences, pp. 695–702.
- [8] WHIPPLE, F. J. W. The stability of the motion of a bicycle. *Quarterly Journal of Pure and Applied Mathematics* 30 (1899), 312–348.

A Measured Bicycle and Rider data

This appendix summarizes the measured geometry and mass data of the bicycles and rider used. The first bicycle is the Stratos which can be characterized as a hybrid bicycle. The second bicycle is the Browser which is a standard Dutch city bicycle.

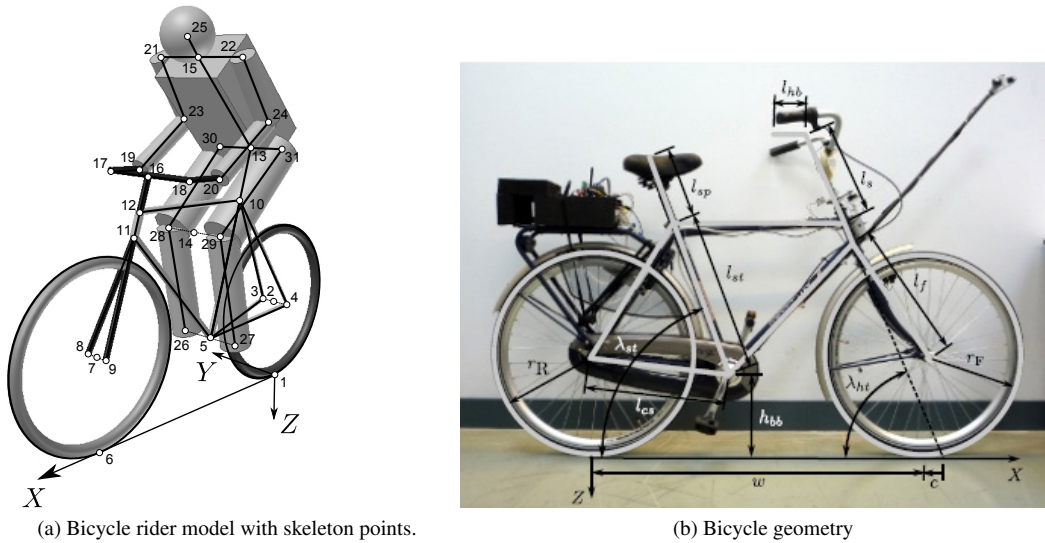


Figure 6: **a)** Bicycle rider model with skeleton points and **b)** bicycle geometry.

Parameter	Symbol	Value for Stratos	Value for Browser
Bottom bracket height	h_{bb}	0.290 m	0.295 m
Chain stay length	l_{cs}	0.445 m	0.460 m
Fork length	l_f	0.455 m	0.455 m
Front hub width	w_{fh}	0.100 m	0.100 m
Handlebar length	l_{hb}	-0.090 m	0.190 m
Rear hub width	w_{rh}	0.130 m	0.130 m
Seat post length	l_{sp}	0.195 m	0.240 m
Seat tube angle	λ_{st}	75.0°	68.5°
Seat tube length	l_{st}	0.480 m	0.530 m
Stem length	l_s	0.190 m	0.250 m
Wheel base	w		see Table 1
Trail	c		see Table 1
Head tube angle	$\lambda_{ht} = 90^\circ - \lambda$		see Table 1
Rear wheel radius	r_R		see Table 1
Front wheel radius	r_F		see Table 1

Table 1: Bicycle geometry dimensions for the Stratos and the Browser bicycle according to figure 6b.

<u>Parameter</u>	<u>Symbol</u>	<u>Value for Stratos</u>	<u>Value for Browser</u>
Wheel base	w	1.037 m	1.121 m
Trail	c	0.0563 m	0.0686 m
Steer axis tilt	λ	16.9°	22.9°
Gravity	g	9.81 N/kg	9.81 N/kg
Forward speed	v	<i>various</i> m/s	<i>various</i> m/s
Rear wheel R			
Radius	r_R	0.338 m	0.341 m
Mass	m_R	3.96 kg	3.11 kg
Inertia	(I_{Rxx}, I_{Ryy})	(0.0916, 0.1545) kgm ²	(0.0884, 0.1525) kgm ²
Rear Body and frame assembly B			
Centre of mass	(x_B, z_B)	(0.3267, -0.4825) m	(0.2799, -0.5348) m
Mass	m_B	7.22 kg	9.86 kg
Inertia	$\begin{bmatrix} I_{Bxx} & 0 & I_{Bxz} \\ 0 & I_{Byy} & 0 \\ I_{Bxz} & 0 & I_{Bzz} \end{bmatrix}$	$\begin{bmatrix} 0.37287 & 0 & -0.03835 \\ 0 & 0.71687 & 0 \\ -0.03835 & 0 & 0.45473 \end{bmatrix}$ kgm ²	$\begin{bmatrix} 0.52714 & 0 & -0.11442 \\ 0 & 1.31761 & 0 \\ -0.11442 & 0 & 0.75920 \end{bmatrix}$ kgm ²
Front Handlebar and fork assembly H			
Centre of mass	(x_H, z_H)	(0.9089, -0.7296) m	(0.8632, -0.7467) m
Mass	m_H	3.04 kg	3.22 kg
Inertia	$\begin{bmatrix} I_{Hxx} & 0 & I_{Hxz} \\ 0 & I_{Hyy} & 0 \\ I_{Hxz} & 0 & I_{Hzz} \end{bmatrix}$	$\begin{bmatrix} 0.17684 & 0 & -0.02734 \\ 0 & 0.14443 & 0 \\ -0.02734 & 0 & 0.04464 \end{bmatrix}$ kgm ²	$\begin{bmatrix} 0.25338 & 0 & -0.07205 \\ 0 & 0.24537 & 0 \\ -0.07205 & 0 & 0.09558 \end{bmatrix}$ kgm ²
Front wheel F			
Radius	r_F	0.340 m	0.344 m
Mass	m_F	3.334 kg	2.02 kg
Inertia	(I_{Fxx}, I_{Fyy})	(0.09387, 0.15686) kgm ²	(0.0904, 0.1494) kgm ²

Table 2: Parameters for the Stratos and the Browser bicycle for the bicycle model from figure 2.

<u>Parameter</u>	<u>Symbol</u>	<u>Rider1</u>
Chest circumference	c_{ch}	0.94 m
Forward lean angle	λ_{fl}	63.9° (on Stratos) 82.9° (on Browser)
Head circumference	c_h	0.58 m
Hip joint to hip joint	l_{hh}	0.26 m
Lower arm circumference	c_{la}	0.23 m
Lower arm length	l_{la}	0.33 m
Lower leg circumference	c_{ll}	0.38 m
Lower leg length	l_{ll}	0.46 m
Shoulder to shoulder	l_{ss}	0.44 m
Torso length	l_{to}	0.48 m
Upper arm circumference	c_{ua}	0.30 m
Upper arm length	l_{ua}	0.28 m
Upper leg circumference	c_{ul}	0.50 m
Upper leg length	l_{ul}	0.46 m
Rider mass	m_{Br}	72.0 kg
Head mass	m_h	0.068 m_{Br}
Lower arm mass	m_{la}	0.022 m_{Br}
Lower leg mass	m_{ll}	0.061 m_{Br}
Torso mass	m_{to}	0.510 m_{Br}
Upper arm mass	m_{ua}	0.028 m_{Br}
Upper leg mass	m_{ul}	0.100 m_{Br}

Table 3: Anthropomorphic data for rider A according to figure 6a.

```

%% Matlab code for Skeleton Grid Points see Figure 1b
%% Adapted Table 10 from MooreHubbardKooijmanSchwab2009
r1 = [0 0 0];
r2 = [0 0 -rR];
r3 = r2 + [0 wrh/2 0];
r4 = r2 + [0 -wrh/2 0];
r5 = [sqrt(lcs^2-(rR-hbb)^2) 0 -hbb];
r6 = [w 0 0];
r7 = r6 + [0 0 -rF];
r8 = r7 + [0 wfh/2 0];
r9 = r7 + [0 -wfh/2 0];
r10 = r5 + [-lst*cos(last) 0 -lst*sin(last)];
% calculate f0
f0 = rF*cos(laht)-c*sin(laht);
r11 = r7 + [-f0*sin(laht)-sqrt(lf^2-f0^2)*cos(laht) 0 f0*cos(laht)-sqrt(lf^2-f0^2)*sin(laht)];
r12 = [r11(1)-(r11(3)-r10(3))/tan(laht) 0 r10(3)];
r13 = r10 + [-lsp*cos(last) 0 -lsp*sin(last)];
% determine mid knee angle and mid knee position
a1 = atan2((r5(1)-r13(1)), (r5(3)-r13(3)));
l1 = sqrt((r5(1)-r13(1))^2+(r5(3)-r13(3))^2);
a2 = acos((l1^2+lul^2-lll^2)/(2*l1*lul));
%
r14 = r13 + [lul*sin(a1+a2) 0 lul*cos(a1+a2)];
r15 = r13 + [lto*cos(laf1) 0 -lto*sin(laf1)];
r16 = r12 + [-ls*cos(laht) 0 -ls*sin(laht)];
r17 = r16 + [0 lss/2 0];
r18 = r16 + [0 -lss/2 0];
r19 = r17 + [-lhb 0 0];
r20 = r18 + [-lhb 0 0];
r21 = r15 + [0 lss/2 0];
r22 = r15 + [0 -lss/2 0];
% determine left elbow position
a1 = atan2((r19(1)-r21(1)), (r19(3)-r21(3)));
l1 = sqrt((r19(1)-r21(1))^2+(r19(3)-r21(3))^2);
a2 = acos((l1^2+lua^2-lla^2)/(2*l1*lua));
%
r23 = r21 + [lua*sin(a1-a2) 0 lua*cos(a1-a2)];
r24 = r23 + [0 -lss 0];
r25 = r15 + [ch/(2*pi)*cos(laf1) 0 -ch/(2*pi)*sin(laf1)];
r26 = r5 + [0 lhh/2 0];
r27 = r5 + [0 -lhh/2 0];
r28 = r14 + [0 lhh/2 0];
r29 = r14 + [0 -lhh/2 0];
r30 = r13 + [0 lhh/2 0];
r31 = r13 + [0 -lhh/2 0];

```

Table 4: Skeleton points code according to Figure 6a and 6b.